THE PUBLISHING HOUSE
OF THE ROMANIAN ACADEMY

PROCEEDINGS OF THE ROMANIAN ACADEMY, Series A,
Volume 20, Number 4/2019, pp. 353–360

EXPERIMENTAL STUDY OF TERAHERTZ RESPONSE FROM SOME FERROELECTRIC AND DIELECTRIC MATERIALS

M. G. BANCIU[1], L. NEDELCU[1], T. FURUYA[2], L. HRIB[1], D. C. GEAMBASU[1], L. TRUPINA[1], D. PANTELICA[3], M.-D. MIHAI[3], M. TANI[2]

[1] National Institute of Materials Physics, Magurele, Jud. Ilfov, Romania
[2] Research Center for Development of Far-Infrared Region, University of Fukui, Fukui, Japan
[3] "Horia Hulubei" National Institute for Research and Development in Physics and Nuclear Engineering, Magurele, Jud. Ilfov, Romania
Corresponding author: Marian Gabriel BANCIU, E-mail: gbanciu@infim.ro

Abstract. Barium strontium titanate (BST) ferroelectric layers were deposited on high resistivity Si substrates by Pulsed Laser Deposition and Radio Frequency sputtering. The stoichiometry was measured by using the Rutherford Backscattering technique at 3.041 MeV. For sub-THz measurements of Si samples, a new resonant method placing the sample between two flanged waveguides is proposed. In the THz range, the Time Domain Spectroscopy proved to be a reliable method. Both methods show effects due to the dielectric losses of BST in that frequency range.

Key words: Terahertz, barium strontium titanate, time domain spectroscopy.

1. INTRODUCTION

Terahertz systems exhibit particular characteristics mainly due the position of the THz radiation between microwaves (electronic domain) and infrared (photonic domain) [1,2]. In the last decade, Terahertz technologies rapidly evolved providing attractive solutions for imaging, drug identification, sensing etc. Despite the very short period since the "THz gap" was actually filled, THz technologies has provided mature and powerful investigation techniques [3,4]. In addition, due to the scarcity of electromagnetic spectrum resources, THz offer solutions for high speed communications. The demand of devices and systems at Terahertz frequencies was continuously increasing in the last years. In the search for improved solutions at these frequencies, advanced dielectrics and ferroelectrics play a significant role.

At higher frequencies, Terahertz Time-Domain Spectroscopy (THz TDS) provides accurate direct measurements of both amplitude and phase, which is far more convenient compared to other methods as Fourier Transform Infrared Spectroscopy (FTIR). Femtolasers with pulses shorter than 10 fs excited THz waves in the bow-tie H shaped antennas on GaAs with a spectrum up to 7 THz in special conditions [5]. In addition, THz TDS systems with a significant increase in measurement speed were reported [6].

A special attention to the sub-Terahertz measurement techniques is given in this work. Despite the success of some research groups in proposing different kinds of methods to characterize dielectrics [7], the methods in sub-Terahertz range are less robust than THz TDS. Due to this aspect, the material data show a gap between microwaves, where reliable resonant techniques are available and THz, where the data are provided in most of the cases by the time domain spectroscopy. Fabrication of very large samples showing uniformity required by free space measurement methods at sub-THz frequencies is a real challenge for material scientists. In addition, for accurate measurements, the sample thickness should be comparable with the wavelength of the sub-THz waves. In this work, for the sub-THz range, we will employ a transmission/reflection method with the dielectric sample placed between two flanged waveguides as in [8]. In Section 3 we present our resonant method, which uses a similar setup as [8] and [9]. The method presented in [9] is also resonant, but, as we will show in Section 3, it differs from our method because the model used in [9] for waveguide-flanged cavity response is that of a generalized Fabry-Perot resonator, while our method considers the sample as a dielectric rectangular resonator.

2. PREPARATION OF BARIUM STRONTIUM TITANATE CERAMICS AND FILMS

The barium strontium titanate $(Ba_{1-x}Sr_x)TiO_3$ (BST) is a ferroelectric material, which offers features in microwaves notably for agile devices [10]. In most of the cases $x = 0.4$, because this composition is very attractive for applications at room temperature. In this work, ceramic targets for pulsed laser deposition (PLD) and for RF magnetron sputtering were manufactured and BST films were deposited on 525 μm thick silicon from Topsil with 20 kΩ cm resistivity.

Ceramic targets were manufactured in the laboratory by using conventional solid-state reaction technique in order to be used for BST films depositions. The fabrication process was previously described [11]. For this work, the optimization of the sintering temperature was required. This was performed by analysis of the dielectric parameters of BST samples sintered at various temperatures as shown in Fig. 1. The dielectric parameters in Fig. 1 were measured at 1 kHz. As it can be observed, sintering at the higher temperature of 1400 ^{o}C offers both a higher dielectric constant and lowers dielectric losses at room temperature.

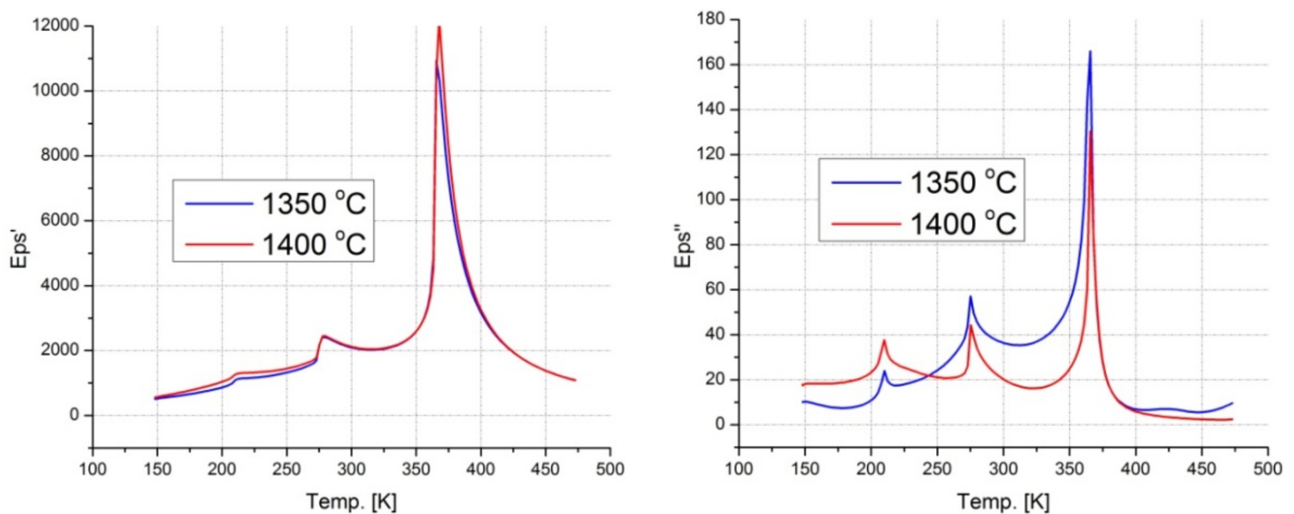

Fig. 1 – Dielectric characteristics versus temperature of BST ceramics ($x = 0.1$) for two sintering temperatures 1350 ^{o}C and 1400 ^{o}C. Real value of the dielectric permittivity (left); immaginary value of the dielectric permittivity (right).

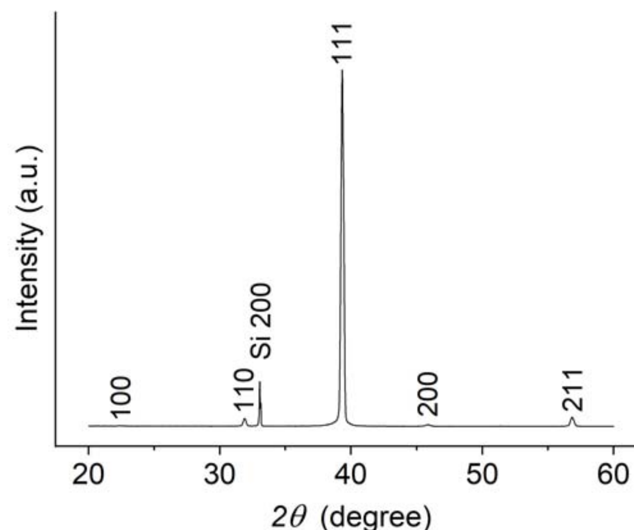

Fig. 2 – X-ray diffraction pattern of a BST film with 40% Sr content deposited using PLD on high resistivity (100) Si.

Two methods were used for BST films deposition: Pulsed Laser Deposition (PLD) and radio-frequency (RF) sputtering. For the film prepared by PLD it was used a pulsed KrF laser with $\lambda = 248$ nm focused on the

BST target at an angle of 45°. The laser repetition rate and fluence used for deposition were 5 Hz and 2 J/cm^2, respectively. During ablation, in order to achieve a high degree of film crystallinity and to avoid oxygen vacancy formation, the substrate temperature was set to 700 °C while the oxygen partial pressure was 0.15 mbar. The Scanning Electron Microscopy (SEM) investigations put in evidence the columnar grow for the BST layers deposited by using PLD as shown in Fig. 3. The roughness of BST layers deposited via PLD was investigated by using atomic force microscopy (AFM) as shown in Fig. 4.

For the RF sputtering, the BST thin films were grown from BST ceramic targets by reactive radio-frequency sputtering method using an ULVAC SBR-1102E system. The sputtering chamber was pumped down to 10^{-6} torr before admission of sputtering gases. Next, high purity working gas mixture (90% of argon and 10% oxygen) was introduced and the total pressure was adjusted to 3×10^{-2} torr. 300 nm thick films were grown on heated silicon substrates at 600 °C and an applied RF power density of 5.1 W/cm^2.

The BST layers deposited via RF sputtering showed an increased smoothness. However, the RF sputtering of barium strontium titanate required an increased attention to the stoichiometry. The Curie temperature for BST decreases with the increase of strontium content x. At room temperature, a small variation in x can significantly modify the dielectric and transmitting properties of BST.

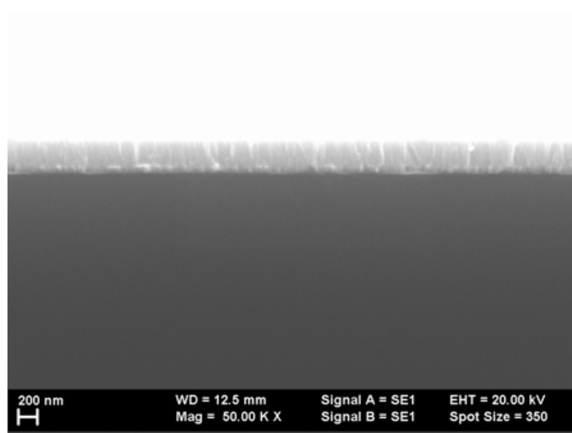

Fig. 3 – SEM image of a BST film with 40% Sr content deposited by using PLD on high resistivity Si substrate.

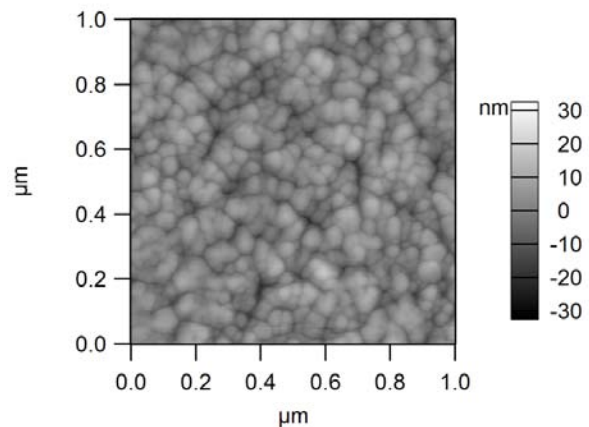

Fig. 4 – Atomic Force Microscopy of the BST film obtained by Pulsed Laser Deposition.

In order to control the BST layer stoichiometry, the samples were investigated by employing the Rutherford Backscattering Spectrometry method (RBS). Measurements were performed using a 3.041 MeV $^4He^{++}$ particle beam from the 3.0 MV Tandetron accelerator at the IFIN-HH Institute in Bucharest-Magurele. The beam was extracted from the duo-plasmatron ion source. The energy of backscattered particles was measured by a ORTEC silicon detector placed at 165°. For the sample PRO10 deposited by PLD, 600 nm thick BST film, the RBS measurements shown in Fig. 5 showed that the film preserves the stoichiometry of the target. Hence the strontium content was $x = 0.4$ in both ceramic target and deposited film. However, for the sample P53U deposited by RF sputtering, the RBS data are shown in Fig. 6 and the element concentration is given in Table 1.

Table 1

Results of the RBS measurements on the RF sputtered BST film (sample P53U)

Number of Layer	Found element and concentration				Thickness (atoms × 10^{15} /cm^2)
1	Ba 0.68	Sr 0.32	Ti 0.9	O 2.4	3000
2	Si 1				infinity

The sample discussed in Table 1 was deposited by RF sputtering from BST target with $x = 0.25$ Sr content. This difference in stoichiometry can be explained by the phenomena of preferential sputtering, elements with different atomic mass or binding energy strength being sputtered at different rates, hence the

difference in stoichiometry. The RBS measurements showed that, for a required $x=0.4$ Sr content in the film obtained by Radio Frequency sputtering, a target with $x\sim0.33$ should be used.

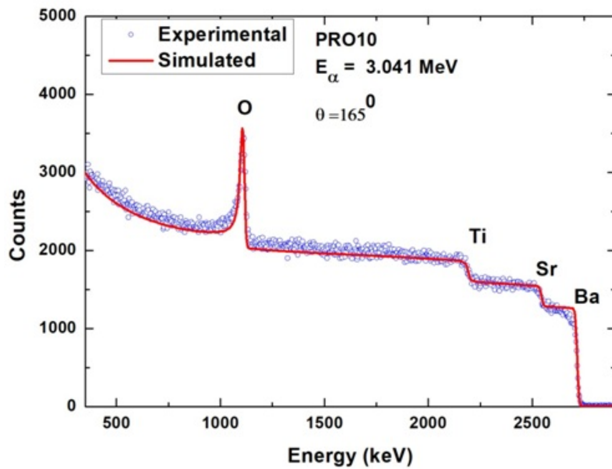

Fig. 5 – Rutherford Back-Scattering spectra on a BST film ($x=0.4$) deposited on Si by Pulsed Laser Deposition.

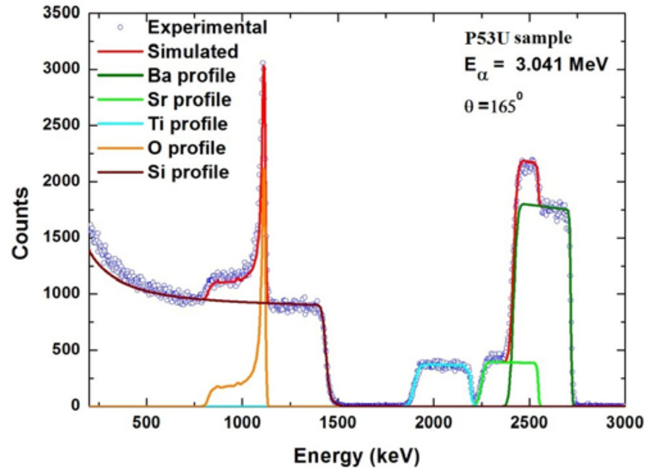

Fig. 6 – Rutherford Back-Scattering spectra on a BST film ($x=0.32$) deposited on Si by RF sputtering.

3. MILLIMETER WAVE MEASUREMENT SETUP WITH TWO FLANGED WAVEGUIDES

For measuring dielectric properties in the 75–110 GHz band, the waveguide transmission/reflection methods, which are successfully applied in microwaves cannot be used due to difficulty of shaping the material sample in order to accurately fit such small section as 2.54 mm by 1.27 mm of the of the WR-10 rectangular waveguide. For measurements in sub-THz range, we used a simple setup with the sample between two flanged rectangular waveguides [8].

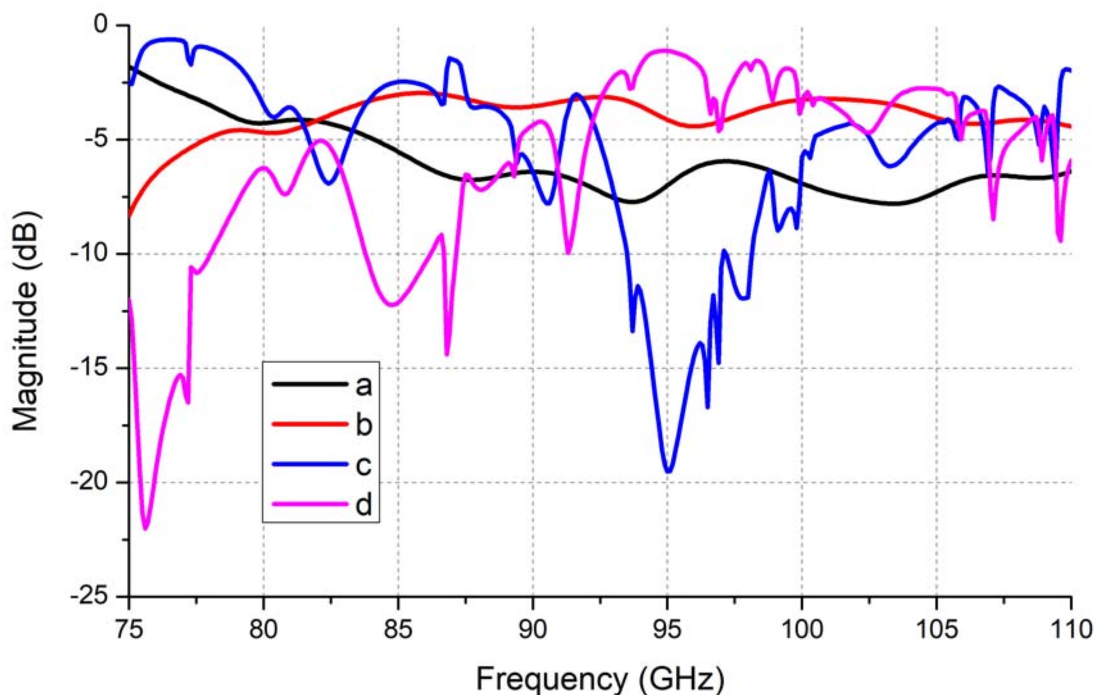

Fig. 7 – Scattering parameters for 5 mm × 5 mm × 0.525 mm samples in a transmission setup: a) magnitude of S_{21} for Teflon sample, b) magnitude of S_{11} for Teflon sample, c) magnitude of S_{21} for Si sample, d) magnitude of S_{11} for Si sample.

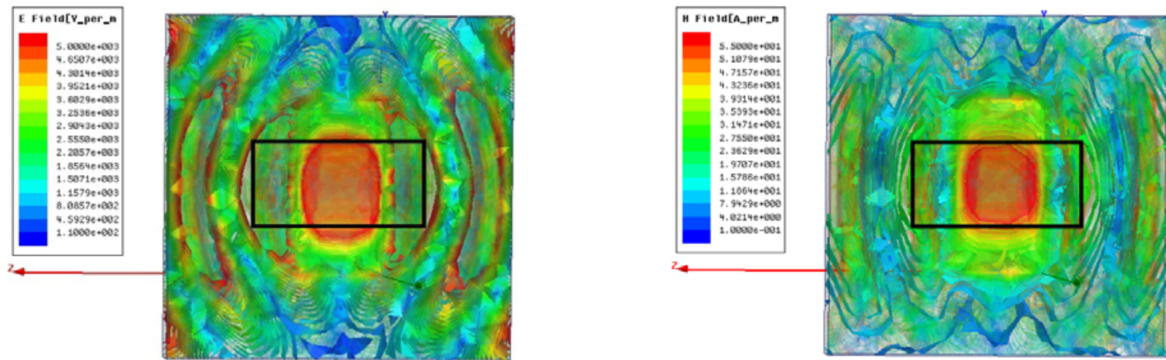

Fig. 8 – Electric field (left) and magnetic field (right) distribution in a Teflon sample at 103.3 GHz. The black rectangle indicates the WR-10 waveguide aperture.

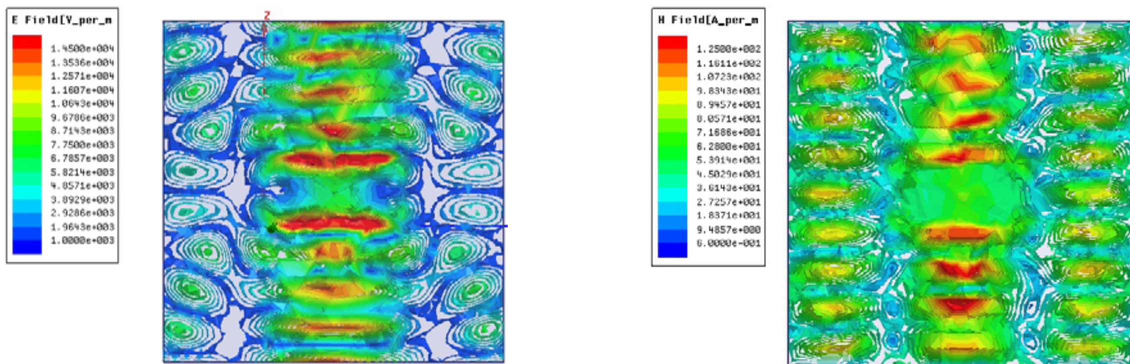

Fig. 9 – Electric field (left) and magnetic field (right) distribution in a Si sample at 82.4 GHz.

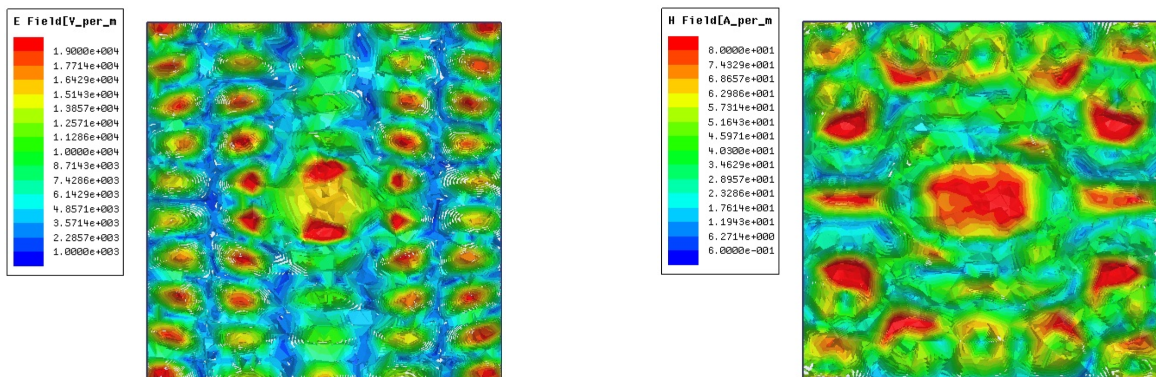

Fig. 10 – Electric field (left) and magnetic field (right) distribution in a Si sample at 90.5 GHz.

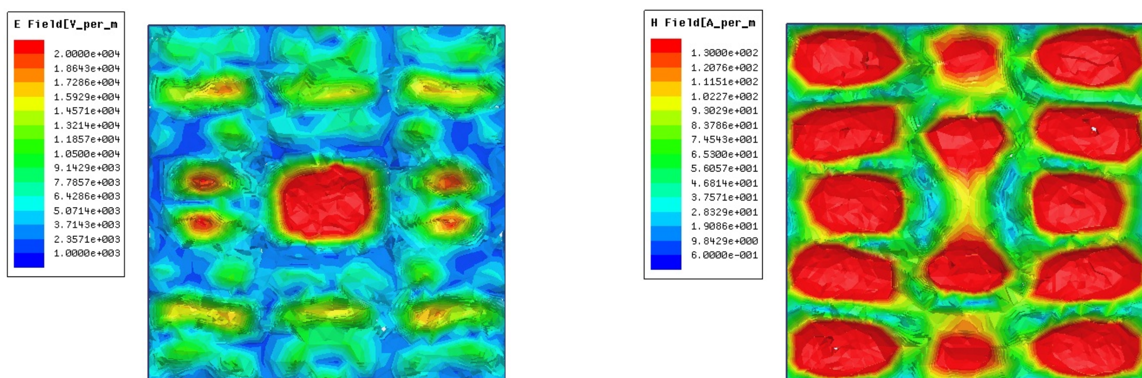

Fig. 11 – Electric field (left) and magnetic field (right) distribution in a Si sample at 99.8 GHz.

For the simple transmission setup in sub-Terahertz range, the dielectric sample to be investigated is placed between the round flanges of two rectangular WR-10 waveguides. For a low dielectric constant sample such as Teflon, the frequency response shown in Fig. 7 does not exhibit any resonances. Full-wave simulations by using HFSS software [12] were carried out on sub-Terahertz wave propagation through dielectric samples. For simulations, the driven modal solution type was chosen. The excitation field was given by the fundamental propagation mode TE_{10}. When modeling a dielectric sample, two of its faces are in contact with waveguides flanges and waveguides apertures. However, the electromagnetic field can radiate through the other four narrow faces. Therefore, a radiation box was drawn in order to include the dielectric sample, the flanges and portions of the rectangular waveguides.

Table 2

Dielectric constant calculated in some frequency points

Measured resonance frequency (GHz)	Resonance mode identified from simulations	Calculated value of relative dielectric constant
82.4	TE_{039}	11.93
90.5	TE_{059}	11.64
99.8	TE_{135}	12.1

In the case of Teflon sample, simulations showed that both electric field and magnetic field pattern exhibit maxima at the center of the sample, in the region of the rectangular waveguide aperture as shown in Fig. 8. However, for the Si sample, the frequency response in Fig. 7 shows several resonances. At the same time, at resonance frequencies, the E-field and H-field patterns exhibit maxima at a large distance from the waveguide aperture as shown in Figs. 9-11 for three resonance frequencies. Such resonant behavior makes not possible the application of measurement method described in [8], which is a non-resonant method. Actually, at resonant frequencies, the Si sample behaves as a rectangular dielectric resonator and the dielectric constant can be calculated from the measured resonant frequencies after the identification of the resonance modes.

Larger Si samples, 10 mm × 10 mm × 0.525 mm were also investigated by using the same setup but no significant differences were observed when compared to the smaller samples. They also exhibited resonances as rectangular dielectric resonators. However, in the same frequency band 75–110 GHz, the resonances could be described by modes with higher indices for Oy and Oz directions than for smaller samples.

Under our best knowledge, this work proposes for the first time a measurement method of the dielectric constant for a sample placed between two flanged waveguides considering the sample a rectangular dielectric resonator. The calculated values of the dielectric constant at some resonance frequencies are presented in Table 2. The values obtained for dielectric permittivity are fairly closed to the expected value of 11.9 of high resistivity Si.

The experiments on Si samples with BST deposited did not show significant change in the resonant frequencies due to the small thickness of the BST layer. However, some decrease in the magnitude of S_{21} response could be noticed due to the dielectric loss of the BST layer.

4. TERAHERTZ TIME DOMAIN SPECTROSCOPY

The Terahertz Time Domain Spectroscopy proved to be very effective for characterization of dielectric materials with high dielectric constant and low dielectric losses [13, 14].

The high resistive Si substrate is actually one of the most transparent materials in THz and is used to show the bandwidth of the THz TDS system [5] as in Fig. 12. The ripple of the transmission curve of Si is due to the Fabry-Perot effect, i.e. it represents the multiple reflections of the THz wave in the Si plate.

The 200 nm thick BST layer deposited on high resistivity Si was investigated by using THz Time Domain Spectroscopy. The waveforms in time-domain for the reference signal, for the signal through a silicon substrate without any deposition and for the signal through BST film on Si substrate are shown in Fig. 13. It can be seen that the delay of the main peak and of the multiple reflections of the BST film on silicon, are mainly due to the Si substrate. The Si substrate exhibits a dielectric constant about 11.9, which is much lower than the dielectric permittivity of the BST layer. However, the Si substrate is very thick compared to the film, which explains the observed delay of the peaks.

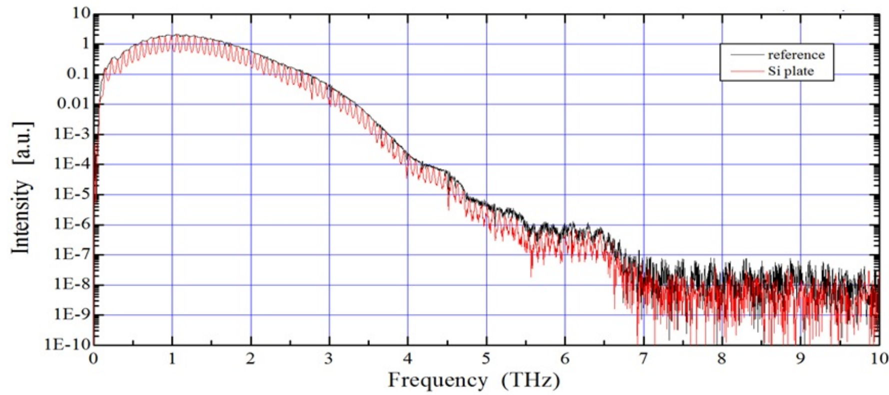

Fig. 12 – THz power spectrum for the reference signal (black) and a 0.5 mm high resistivity Si (red) measured with the Pulse IRS 2000 Pro Time Domain Spectrometer from Aispec [5].

On the other side, the THz spectrum of the BST layer deposited is clearly lower than the spectrum of the Si sample, shown in Fig. 14, only because the significant losses in the ferroelectric material. The variation in thickness for Si substrate given by the manufacturer is about ±2 μm, which is higher than the thickness of the BST film. Therefore, for accurate measurements, the same Si substrate used for BST deposition must be measured by using THz TDS before the BST deposited on the substrate is measured. In addition, in order to increase the method accuracy, BST films with an increased thickness are required for measurements.

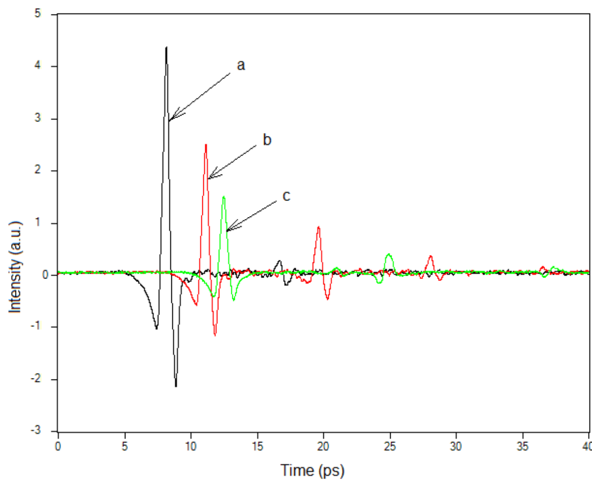

Fig. 13 – Time domain pulses during the measurements of BST film on Si substrate: a) reference; b) Si substrate only; c) BST film deposited on Si substrate.

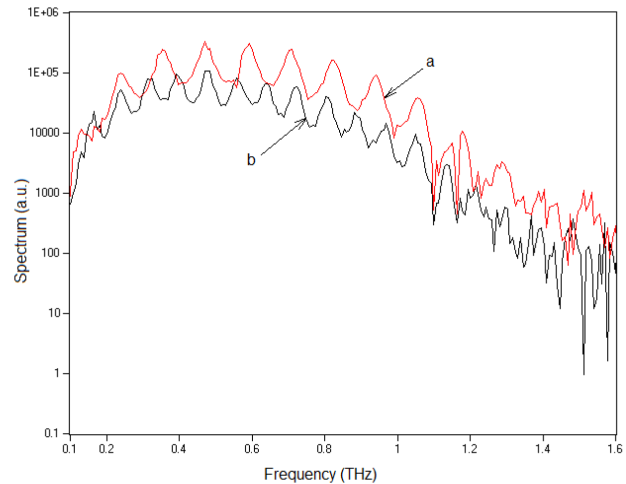

Fig. 14 – THz spectrum for the BST film on Si substrate (b) compared to the spectrum for Si substrate without deposition (a).

5. CONCLUSIONS

Terahertz and sub-Terahertz investigation methods of dielectric substrates and $(Ba_{1-x}Sr_x)TiO_3$ ferroelectric layers deposited on high resistivity Si are discussed in this work. For BST ceramic target preparation, sintering temperature of 1400 °C was chosen because the samples exhibit higher permittivity and lower losses at room temperature than samples sintered at lower temperature.

Two deposition methods were employed for manufacturing BST films on high resistivity silicon substrates. The Rutherford Backscattering Scattering experiments showed that, while the Pulsed Laser Deposition preserves the stoichiometry, the BST layer deposited by Radio Frequency sputtering exhibits a smaller Sr content than for the target.

Measurements on Si samples of various sizes in 75–100 GHz range showed many resonances in the frequency response, with maxima of fields far from the waveguide aperture area. According to our best knowledge, it is for the first time when the sample between the flanged waveguides is considered a dielectric

rectangular resonator and the dielectric constant is calculated after the identification of the resonance modes. The values obtained for dielectric permittivity are fairly closed to the expected ones.

In THz range, the Time Domain Spectroscopy method offers a direct measurement of both the amplitude and phase. The presence of $(Ba_{1-x}Sr_x)TiO_3$ on Si substrate does not significantly change the position in time of the main peaks and of the smaller peaks because the BST thickness is too small. However, the high dielectric losses in BST lead to a important decrease of the measured THz spectrum. In order to increase the measurement accuracy, the substrate used for BST deposition must be firstly characterized in THz before deposition. Moreover, increasing the BST thickness will also increase the accuracy method. In addition, the results at low frequencies (lower than 150 GHz) require a large aperture for a wide THz beam.

Both measurement methods described in this work provide good values for dielectric substrates in their working frequency ranges. However, due to the fact the BST layer is too thin, the methods provide no accurate dielectric parameters for the ferroelectric layer and they are sensitive only to its loss in THz and sub-THz domain.

ACKNOWLEDGEMENTS

This work was partially supported by a grant of the Romanian National Authority for Scientific Research and Innovation, Programme for Space Technology and Advanced Research – STAR, project no. 630 / 2016 MCOATANT, by the TE project No. 134 / 2018, by grants of the Romanian National Authority for Scientific Research and Innovation, CCCDI – UEFISCDI project number 61/2016 (acronym MASTERS) within PNCDI III and by the Core program.

REFERENCES

1. K. SENGUPTA, T. NAGATSUMA, D.M. MITTLEMAN, *Terahertz integrated electronic and hybrid electronic-photonic systems*, Nature Electronics, **1**, pp. 622-635, 2018.
2. D. DRAGOMAN, M. DRAGOMAN, *Terahertz fields and applications*, Progress in Quantum Electronics **28**, *1*, pp. 1-66, 2004.
3. S. DHILLON, M.S. VITIELLO, E.H. LINFIELD, et al., *The 2017 terahertz science and technology roadmap*, Journal of Physics D: Applied Physics, **50**, *4*, p. 043001, 2017.
4. D. SPOREA, L. MIHAI, A. SPOREA, I. VÂȚĂ, *Optical and THz investigations of mid-IR materials exposed to alpha particle irradiation*, Scientific reports, **7**, p. 40209, 2017.
5. ***, AiSPEC , IRS 200 pro, *THz Time-Domain spectrometer – user manual*, 2010.
6. T. FURUYA, E.S. ESTACIO, K. HORITA, C.T. QUE, K. YAMAMOTO, F. MIYAMARU, S. NISHIZAWA, M. TANI, *Fast-scan terahertz time-domain spectrometer based on laser repetition frequency modulation*, Japanese Journal of Applied Physics, **52**, *2R*, p. 022401, 2013.
7. G. ANNINO, M. CASSETTARI, M. MARTINELLI, *Study on planar whispering gallery dielectric resonators. I. General properties*, International, Journal of Infrared and Millimeter Waves, **23**, *4*, pp. 597-615, 2002.
8. M.W. HYDE, M.J. HAVRILLA, *Measurement of complex permittivity and permeability using two flanged rectangular waveguides*, Proceedings of IEEE MTT-S International Microwave Symposium, pp. 531-534, 2007.
9. R. T. SCHERMER, T.H. STIEVATER, *Millimeter-wave dielectric properties of highly refractive single crystals characterized by waveguide resonance*, IEEE Trans. Microw. Theory Techn., **67**, *3*, pp. 1078-1087, 2019.
10. A, GHALEM, M. RAMMAL, L. HUITEMA, A, CRUNTEANU, V. MADRANGEAS, P. DUTHEIRL, F. DUMAS-BOUCHIAT, P. MARCHET, C. CHAMPEAUX, L. TRUPINA, L. NEDELCU, M.G. BANCIU, *Ultra-high tunability of Ba(2/3)Sr(1/3)TiO3-based capacitors under low electric fields*, IEEE Microwave and Wireless Components Letters, **26**, *7*, pp. 504-506, 2016.
11. A. IOACHIM, M.G. BANCIU, L. NEDELCU, *Microwave dielectric properties of doped $(Ba_{0.5}Sr_{0.5})TiO_3$ ceramics correlated with sintering temperature*, J. Optoelectron. Adv. Mater., **7**, *8*, p. 3023-3027, 2005.
12. ***, Ansoft HFSS, v13.0.0, Ansys. Inc., Canonsburg PA, 2011.
13. M.G. BANCIU, L. NEDELCU, K. YAMAMOTO, S. TSUZUKI, M. TANI, *THz TDS investigations on dielectrics for microwave applications.* The 5th International Workshop on Far-Infrared Technologies, Fukui, Japan, March 5-7, 2014.
14. M.G. BANCIU, L. NEDELCU, H.V. ALEXANDRU, T. FURUYA, M. TANI, *Investigations on dielectric parameters of some ferroelectric materials in Terahertz waves*, Symposium Digest of the Second International Symposium on Frontiers in THz Technology FTT 2015, Hamamatsu, Japan, 30 August – 2 September 2015.

Received April 25, 2019